



HAL
open science

Red Blood Cell AE1/Band 3 Transports in Dominant Distal Renal Tubular Acidosis Patients

Jean-Philippe Bertocchio, Sandrine Genetet, Lydie da Costa, Stephen B. Walsh, Bertrand Knebelmann, Julie Galimand, Lucie Bessenay, Corinne Guitton, Renaud de Lafaille, Rosa Vargas-Poussou, et al.

► **To cite this version:**

Jean-Philippe Bertocchio, Sandrine Genetet, Lydie da Costa, Stephen B. Walsh, Bertrand Knebelmann, et al.. Red Blood Cell AE1/Band 3 Transports in Dominant Distal Renal Tubular Acidosis Patients. *Kidney International Reports*, 2020, 5, pp.348 - 357. 10.1016/j.ekir.2019.12.020 . hal-03490101

HAL Id: hal-03490101

<https://hal.science/hal-03490101>

Submitted on 22 Aug 2022

HAL is a multi-disciplinary open access archive for the deposit and dissemination of scientific research documents, whether they are published or not. The documents may come from teaching and research institutions in France or abroad, or from public or private research centers.

L'archive ouverte pluridisciplinaire **HAL**, est destinée au dépôt et à la diffusion de documents scientifiques de niveau recherche, publiés ou non, émanant des établissements d'enseignement et de recherche français ou étrangers, des laboratoires publics ou privés.



Distributed under a Creative Commons Attribution - NonCommercial 4.0 International License

Title

Red blood cell AE1/Band 3 transports in dominant distal renal tubular acidosis patients

*Corresponding authors

Jean-Philippe Bertocchio, MD, PhD
Renal and metabolic diseases unit, European
Georges Pompidou Hospital
20 rue Leblanc, F-75908 Paris CEDEX, France
Phone: +1-(832)-542-7762
Mail: jpbertocchio@gmail.com
Twitter: @JPBertocchio

Dominique Eladari, MD, PhD
Département de Physiologie et Explorations
Fonctionnelles Rénales, Hôpital Felix Guyon,
CHU de la Réunion
Allée des Topazes, F-97400 Saint Denis,
France
Phone: +262 262 90 66 55
Mail: dominique.eladari@inserm.fr

Authors

Jean-Philippe Bertocchio, MD, PhD^{1,2,3,4*}, Sandrine Genetet, PhD^{5,6}, Lydie Da Costa, MD, PhD^{5,7,8},
Stephen B. Walsh, MD, PhD⁹, Bertrand Knebelmann, MD, PhD¹⁰, Julie Galimand⁸, Lucie Bessenay,
MD¹¹, Corinne Guitton, MD¹², Renaud De Lafaille, MD, PhD¹³, Rosa Vargas-Poussou, MD, PhD^{3,14,15},
Dominique Eladari, MD, PhD^{16,17,‡}, Isabelle Mouro-Chanteloup, PhD^{5,6,‡}

‡ contributed equally to this work

Affiliations

- ¹ Assistance Publique-Hôpitaux de Paris, Hôpital Européen Georges Pompidou, Département de Physiologie, F-75015 Paris, France
- ² Université Paris Descartes, Faculté de Médecine, F-75006 Paris, France
- ³ Centre de Référence des Maladies Rénales Héritaires de l'Enfant et de l'Adulte (MARHEA), F-75015 Paris, France
- ⁴ Genito-urinary Medical Oncology and Research department, MD Anderson Cancer Center, 77030, Houston, TX
- ⁵ Université de Paris, UMR_S1134, BIGR, Inserm, F-75015 Paris, France
- ⁶ Institut National de la transfusion sanguine, F-75015 Paris, France
- ⁷ UMR_S1134, Inserm, F-75015 Paris, France
- ⁸ Assistance Publique-Hôpitaux de Paris, Hôpital Robert Debré, service d'Hématologie Biologique, F-75019 Paris, France
- ⁹ University College London Medical School, Royal Free Campus and Hospital, UCL Centre for Nephrology, London, UK
- ¹⁰ Assistance Publique-Hôpitaux de Paris, Hôpital Necker-Enfants malades, Service de Néphrologie, F-75015 Paris, France
- ¹¹ CHU Clermont-Ferrand, Service de Pédiatrie, Clermont-Ferrand, FR
- ¹² Assistance Publique-Hôpitaux de Paris, Hôpital Bicêtre, Service de Pédiatrie, 94 270 Le Kremlin Bicêtre, France
- ¹³ CHU de Bordeaux, Service de Néphrologie, Bordeaux, Aquitaine, FR
- ¹⁴ INSERM, UMRS1138, Centre de Recherche des Cordeliers, F-75006 Paris, France
- ¹⁵ Assistance Publique-Hôpitaux de Paris, Hôpital Européen Georges Pompidou, Service de Génétique, F-75015 Paris, France
- ¹⁶ CHU de la Réunion, Hôpital Felix Guyon, Département de Physiologie et Explorations Fonctionnelles Rénales, F-97400 Saint Denis, France
- ¹⁷ INSERM, UMRS 1283 - European Genomic Institute for Diabetes, F59000, Lille, France

Running headline

HCO₃⁻/Cl⁻ transports in RBC from dRTA patients

Keywords

Acidosis, Renal Tubular; Anion Exchange Protein 1, Erythrocyte; Hematologic Diseases; Nephrocalcinosis; Nephrolithiasis

Word count: 3 686

Abstract

Introduction. Anion exchanger 1 (AE1) (*SLC4A1* gene product) is a membrane protein expressed in both kidney and Red Blood Cells (RBC): it exchanges extracellular bicarbonate (HCO_3^-) for intracellular chloride (Cl^-) and participates to acid-base homeostasis. AE1 mutations in kidney α -intercalated cells can lead to distal renal tubular acidosis (dRTA). In RBC, AE1 (known as Band 3) is also implicated in membrane stability: deletions can cause South Asian Ovalocytosis (SAO).

Methods. We retrospectively collected clinical and biological data from patients harboring dRTA due to a *SLC4A1* mutation and analyzed HCO_3^- and Cl^- transports (by stopped-flow spectrophotometry) and expression (by both flow cytometry, FACS, and Coomassie blue staining) in RBC, as well as RBC membrane stability (ektacytometry).

Results. Fifteen patients were included: All experienced nephrolithiasis and/or nephrocalcinosis, 2 had SAO and dRTA (dRTA SAO+), 13 dominant dRTA (dRTA SAO-). The latter did not exert specific RBC membrane anomalies. Both HCO_3^- and Cl^- transports were lower in dRTA SAO+ than in dRTA SAO- or controls. Using 3 different extracellular probes, we report a decreased expression (by 52%, $p < 0.05$) in dRTA SAO+ by FACS while total amount of protein was not affected. **Conclusion.** Band 3 transport function and expression in RBC from dRTA SAO- patients is normal. However, in SAO RBCs, impaired conformation of AE1/Band 3 corresponds to an impaired function. Thus, the driver of acid-base defect during dominant dRTA is probably an impaired membrane expression.

Keywords

Acidosis, Renal Tubular; Anion Exchange Protein 1, Erythrocyte; Hematologic Diseases; Nephrocalcinosis; Nephrolithiasis

INTRODUCTION

The anion exchanger type 1 (AE1 or Band 3) is an integral membrane protein that exchanges intracellular bicarbonate (HCO_3^-) for extracellular chloride (Cl^-)¹. It is encoded by the *SLC4A1* gene that produces two isoforms: One expressed in the red blood cell (RBC), also known as Band 3, and one expressed in α -intercalated cells (α -ICs) of the renal collecting duct (kAE1) which lacks 65 N-terminal amino-acids². *SLC4A1* gene mutations have been reported to cause either RBC or renal abnormalities. In RBCs membrane, Band 3 that represents about 30% of the total amount of proteins is part of a protein complex that plays an important role in the stability of RBC structure^{3,4}. *SLC4A1* mutations affecting RBCs provoke abnormalities like ovalocytosis or spherocytosis⁵. In the kidney, the main role of kAE1 is to extrude HCO_3^- at the basolateral membrane of α -ICs, which is a critical step for renal acidification. When impaired, intracellular HCO_3^- accumulates that blocks intracellular generation of protons and HCO_3^- from CO_2 and this, ultimately, inhibits apical proton secretion by the v-H⁺-ATPase⁶. Accordingly, *SLC4A1* mutations affecting kAE1 lead to type 1 distal renal tubular acidosis (dRTA), characterized by abnormal proton secretion^{7,8}. It is not known whether kAE1, like its RBCs' homolog Band 3, plays a role as an anchoring structural protein. However, kAE1 has been described to be part of a protein macro-complex involving ankyrin⁹.

How *SLC4A1* mutations affect HCO_3^- transport in kidney is not completely understood. Based on heterologous expression studies in cell models or in *Xenopus* oocytes, some mutations have been proposed to provoke a mistargeting of the protein to the apical membrane, while others are thought to alter intrinsic transport properties of the protein, or to provoke an intracellular retention of the protein^{1,2}. However, it is difficult to draw firm conclusions from these studies because the protein was not expressed in its natural environment. Furthermore, some experiments testing the effects of a mutation have yielded different results when the protein was expressed in different cell models. Indeed, a recent study in a mouse *knock-in* model with the p.R607H mutation, corresponding to p.R589H in Humans, reported different results¹⁰. Interestingly, since kAE1 is a truncated isoform of RBCs' AE1, all mutations affecting kAE1 also affect Band 3. Taking advantage of this, we tested in RBC the effects of *SLC4A1* mutations found in dRTA patients. We measured $\text{Cl}^-/\text{HCO}_3^-$ transports, and AE1/Band 3 surface expression, as well as the RBC structural stability. Finally, we found that patients with dominant dRTA had both normal AE1 expression and function in RBCs, whereas those with recessive dRTA had both important morphological and functional anomalies.

METHODS

Population. All patients came from the European Georges Pompidou Hospital (Paris, France) and the Royal Free Hospital (London, United Kingdom). All (and parents if <18years-old) gave his/her informed consent. All experiments were performed in accordance with relevant guidelines and regulations, as well as the Declaration of Helsinki. All samples were collected in the INTS-CNRGS biobank, approved by the local ethic committee (CPP Ile-de-France II) and the French Research Ministry (ref. DC-2016-2872). Birth date, gender, clinical data at diagnosis, and biological data at diagnosis were collected retrospectively anonymously in accordance to the French regulatory board (ref. 2097359v0).

Red blood cell indices, reticulocyte count, and biochemistry analyses. All EDTA blood samples were immediately shipped at +4°C. A blood smear was provided to avoid artefacts (echinocytes, acanthocytes, spiculated dense red cells). Routine RBC indices were centrally obtained for each sample using a Sysmex auto-analyzer (XN 5000, Sysmex, Kobe, Japan). Blood smear were carefully screened by two independent cytologists who validated RBC morphology anomalies after May-Grünwald Giemsa coloration (MGG).

Ektacytometry. One hundred μL of blood from each patient were run on an ektacytometer (LoRRca MaxSis, RR Mechatronics®, Hoorn, The Netherlands) ^{5, 11}. Each patient was compared to an age-matched healthy control and to the reference values from the laboratory (R. Debré Hospital, Paris, France). Fresh blood was exposed to a shear stress and to an osmotic gradient. The laser beam diffraction pattern through the suspension was detected with a video camera. RBC shapes changed from circular to elliptical as shear stress increases. Then, a deformability index (DI) or elongation index (EI) of cells was derived. The deformation of RBC suspended in a viscous aqueous polyvinylpyrrolidone solution at defined values of applied shear stress of 30Pa and at a constant temperature measurement of 37°C is monitored as a continuous function of suspending medium osmolality. The ektacytometry curve pattern and remarkable points were recorded: i) Omin, reflecting the surface area-to-volume ratio, *i.e.* the osmolality at the minimal deformability in hypo-osmolar area, or the osmolality when 50% of the RBC hemolyzed during the regular osmotic resistance test; ii)

Elmax, corresponding to the maximal DI or EI; and iii) The hyper point or Ohyper, corresponding to the osmolality at half of the DImax or Elmax, *i.e.* the hydration state of the RBC.

Cl⁻/HCO₃⁻ exchanger activity measurements. Three hundred μ L of blood were washed three times in PBS. Washed RBCs were resuspended in 25mL hypotonic lysis buffer (7mM KCl, 10mM Hepes, pH 7.2 for HCO₃⁻ transport or 5mM HPO₄, 1mM EDTA, pH 8.0 for Cl⁻ transport) for 40min at +4°C, followed by resealing for 1h at 37°C in resealing buffer (100mM KCl, 10mM Hepes, pH 7.2, 1mM MgCl₂ and 2mg/mL bovine carbonic anhydrase for HCO₃⁻ transport or 50mM KCl, 50mM Hepes, pH 7.2, 1mM MgCl₂ for Cl⁻ transport) containing 0.15mM of the fluorescent pH-sensitive dye pyranine (1-hydroxypyrene-3,6,8-trisulfonic acid, Sigma-Aldrich, St. Louis, MO, USA) for HCO₃⁻ transport, or 2.8mg/mL SPQ probe for Cl⁻ transport (6-methoxy-N-(3-sulfopropyl) Quinolinium, Invitrogen Fisher Scientific, Illkirch, France). After three washes in ice-cold incubation buffer (resealing buffer without MgCl₂ and probe), stopped-flow experiments were performed at 30°C for HCO₃⁻ transport and 20°C for Cl⁻ transport (SFM400; Bio-logic, Grenoble, France) as previously described¹². Excitation was performed at 465nm for HCO₃⁻ transport (365nm for Cl⁻ transport) and emitted light was filtered with a 520nm cut-off filter for HCO₃⁻ transport (450nm for Cl⁻ transport). For measurement of HCO₃⁻/Cl⁻ exchange activity, dye-loaded ghosts resuspended in 3mL “chloride buffer” (100mM KCl and 10mM Hepes pH 7.2 for HCO₃⁻ transport or 50mM KCl, 50mM Hepes, pH 7.2 for Cl⁻ transport) were rapidly mixed with an equal volume of bicarbonate buffer (100mM KHCO₃ and 10mM Hepes, pH 7.2 for HCO₃⁻ transport or 100mM KHCO₃⁻, 200mM sucrose 10mM Hepes, pH 7.2 for Cl⁻ transport), generating an inwardly directed HCO₃⁻/CO₂ gradient of 50mEq/L and an outwardly directed Cl⁻ gradient of equal magnitude. Data from six time courses were averaged and fit to a mono-exponential function using the simplex procedure of Biokine software (Bio-logic, Grenoble, France). It allowed the measurement of a transport constant (k). Then, permeability was calculated as the following equation:

$$(1) P=k*r/3$$

where P is permeability (in μ m.sec⁻¹), k is transport constant (in sec⁻¹), and r is radius (in μ m).

Protein quantification. AE1 surface expression on RBCs was detected using a FACSCanto II flow cytometer (BD BioSciences, Bedford, MA, USA), after glutaraldehyde (0.025%) fixation and staining either with a monoclonal human anti-Diego b (1/4, HIRO 58, provided by Dr. M. Uchikawa, Japanese Red Cross Central Blood Center, Tokyo, Japan) or the mouse monoclonal Bric6 (1/40, IBGRL, Bristol,

UK) antibodies. Secondary antibodies were PE-conjugated goat anti-human and anti-mouse respectively (1/100; Beckman Coulter, Brea, CA, USA). Flow cytometer results were analyzed using FlowJo software (FlowJo, Ashland, OR, USA). Eosin-5'-maleimide (EMA) dye tests have also been performed^{11, 13}. For the Coomassie blue analysis, ghosts were prepared by hypotonic lysis, providing "white" ghosts¹⁴. Membrane proteins from whole ghost cell lysates were separated on SDS-PAGE (4-12% acrylamide) in reducing conditions (2.8 mM β -mercaptoethanol) and stained with Coomassie blue. The densitometric analyses of data were performed using ImageJ 1.46j software.

Ghost diameter measurements. Ghosts preparation was the same as the one for stopped flow experiments except for pyranine concentration (1.5mM). Two percent of ghosts were mounted between slide and coverslip. Ghost diameters were measured using an Axio Observer Z1 microscope with an AxioCam MRm camera (Zeiss, Marly-le-Roi, France). An average of 800 fluorescent ghosts were measured for each genotype.

Statistical analyses. Due to the low number of values in some groups, the distribution could not be supposed as normal. So, we only used non-parametric tests: Mann-Whitney when 2 groups were compared, and the Kruskal-Wallis test (with Dunn's multiple comparison test) when more than 2 groups were compared. Data are presented as their median and interquartile range [Q1-Q3]. We considered a p value <0.05 as significant.

DATA AVAILABILITY STATEMENT

The datasets generated during and/or analyzed during the current study are available from the corresponding author on reasonable request.

RESULTS

Included patients

Fifteen patients were included. **Table 1** shows their characteristics at diagnosis. Seven were diagnosed when they were adults. In children, the earliest diagnosis was performed within the first year of life. Two patients carried the characteristic molecular anomaly associated with South Asian Ovalocytosis (SAO), which corresponds to the in frame deletion of 27 nucleotides of *SLC4A1* gene, leading to the loss of 9 amino acids (**Table 2**). Those 2 patients harbored other *SLC4A1* mutations: one carried the recessive p.G701D mutation involved in dRTA, while the other carried the amino acid change p.E90K, involved in spherocytosis and the p.T581D one, involved in dRTA (**Figure 1**). All other patients carried a missense dominant mutation. Seven in position 589 of the protein: 4 had p.R589H and 3 p.R589C. Three affected dRTA patients harbored missense p.S613F, p.E906*, and p.G609R mutations, while one carried a duplication (p.D905dup). Interestingly, 2 patients exhibited non-reported mutations (p.E906K and p.S525F). According to the guidelines of the American College of Medical Genetics and Genomics ¹⁵, we found 16 of them to be pathogenic or likely pathogenic (class 5 and 4, respectively), while 2 more were of uncertain significance (*i.e.* class 3).

Three patients had chronic kidney disease as defined by an estimated glomerular filtration rate (eGFR) <60 mL/min/1.73m², and 6 had overt metabolic acidosis as defined by [HCO₃⁻] <20 mM. All patients had a history of nephrolithiasis and/or nephrocalcinosis. Six patients did not have a familial history of renal/metabolic injury. Dynamic testing of renal acidification was performed in 8 patients: two had an abnormal Δ U-B(PCO₂) ¹⁶, two others had an abnormal response to the acute acid load test ¹⁷, and 4 more had an abnormal response to the furosemide-fludrocortisone test ¹⁸ (amongst those, 3 had also an abnormal response to the acute acid load test). Bone demineralization was reported in 4 patients.

Routine hematological analysis

No patient exhibited neither overt anemia or other hemoglobinopathy (such as thalassemia or sickle cell disease). All had a normal mean corpuscular volume and none had any anomalies in blood cells counts (**Table 3**) at the time of inclusion. No cytological anomaly was detected in RBCs from dRTA patients without SAO (dRTA SAO-), while we observed the characteristic defects in RBCs from SAO patients (dRTA SAO+): ovalocytes and very large RBCs, exhibiting 1 or two curvilinear transverse strips (**Figure 2**). The RBC deformability (Elmax), surface area-to-volume ratio (Omin) and the

hydration state (Ohyper) of RBC from dRTA SAO⁻ did not significantly differ as compared to controls. As expected, only dRTA SAO⁺ had a large decreased RBC deformability (Elmax) with almost non-measurable ektacytometry parameters (**Table 3** and **Figure 2** lower panel). dRTA SAO⁻ do not exert neither clinical nor biological overt anomalies; moreover, their RBC membranes seem to be comparable to the ones of controls subjects. Only dRTA SAO⁺ exerted severe morphological RBC membrane dysfunction.

Bicarbonate and chloride transports through red blood cells membrane

Figure 3 shows the transport of HCO₃⁻ and Cl⁻ in ghosts. Diameters of ghosts (**Panel A**) obtained after RBC hypotonic lysis and resealing were not significantly different between groups (median 6.25, 5.88, and 7.67 μm in controls, dRTA SAO⁻, and dRTA SAO⁺, respectively), and hence, surfaces of exchange were not significantly different (123, 108, and 185 μm² in controls, dRTA SAO⁻, and dRTA SAO⁺, respectively). Transport constants (k) for HCO₃⁻ (**Panel B**) and Cl⁻ (**Panel C**) were significantly lower in dRTA SAO⁺ as compared to the dRTA SAO⁻ ones. Even though all dRTA SAO⁻ had measurements close to the controls ones, the patient with the p.S525F mutation had k(HCO₃⁻) values very close to the ones measured in dRTA SAO⁺. Taken together, the relative values of k(HCO₃⁻) and k(Cl⁻) allow to distinguish clearly dRTA SAO⁺, while dRTA SAO⁻ are merged within the controls (as plotted in **Panel D**). For the patients in whom we measured surface of exchange, the calculated relative permeabilities (P) were lower in dRTA SAO⁺ than in the dRTA SAO⁻ ones for both HCO₃⁻ and Cl⁻, confirming the distinction between dRTA SAO⁺ to the others (**Panel E**). Thus, dRTA SAO⁻ express an AE1 protein that is capable of normal anion transports, while only dRTA SAO⁺ exhibit severe impairment in AE1-dependent anion exchange.

AE1 expression in red blood cells

To determine if the lower transport activity of AE1 in those patients is related to lower membrane AE1 expression or to an intrinsic transport defect, we quantified its membrane expression (**Figure 4**). We used 3 different probes: EMA, Bric6, and Diego b (**Panel B**) that all recognize extracellular part of the protein. Flow cytometry analysis (**Panel A**) showed a reduced labelling in dRTA SAO⁺ (52%) than in controls (100%, *p*<0.05) or dRTA SAO⁻ (104%) as labelled with EMA, Bric6 (14%), or Diego b (54%).

Noteworthy, the patient with p.S525F mutation exhibited similar values than dRTA SAO⁻ and controls. We also quantified the total amount of protein present in RBC membranes by quantifying the third band (*i.e.* Band 3) by Coomassie blue staining after gel electrophoresis (**Panel C**). No difference was observed between controls, dRTA SAO⁻, and dRTA SAO⁺ for the density of Band 3 ($p = 0.26$) even when Band 3 density was normalized to the density of all polypeptides from same lane ($p = 0.37$) (**Panel D**).

Taken together, the aforementioned results indicate that expression of Band 3 in dRTA SAO⁻ is normal. In dRTA SAO⁺, AE1 membrane expression is decreased whereas the total amount of AE1 protein remains normal.

Finally, we show that only patients with SAO mutation exert severe RBC morphological anomalies with a large decrease in Band 3 transport function that seems to be related to its membrane expression, whereas in dRTA patients without SAO mutation, both functional (transport) and morphological functions are preserved.

DISCUSSION

Taken together, our data show that mutations in *SLC4A1* gene associated with dominant dRTA do not affect the function of the erythroid isoform Band 3 except if the patient has an additional deletion causing SAO. The stopped-flow spectrophotometry analyzes that we report in this context has some limitations. First, to measure the HCO₃⁻ transport, we used an intracellular pH-sensitive probe (pyranine) as a proxy (not the direct HCO₃⁻ concentration): we also report here results with the SPQ probe (measuring Cl⁻ concentration) which results are highly correlated to the ones of pyranine ($r^2=0.62$, $p<0.0001$). Previous reports have also shown similar results in heterologous models (*Xenopus oocytes*)^{19, 20} or using sulfate as a surrogate for chloride transport²⁰. Secondly, the intracellular pH is also depending on the carbonic anhydrase activity: to blunt this limiting step, we saturated the intracellular compartment with 2 mg/mL of bovine carbonic anhydrase in every ghost. Finally, the systemic acidosis could impair the function of the AE1 protein: of note, patients with the most (acidotic) phenotype (at least at diagnosis) were not the ones carrying a SAO mutation. Nonetheless, this is the first report of in-depth assessment of RBC membrane disorders in patients with AE1-related dRTA. Very recently, an international cohort of dRTA patients was reported with many data on both the phenotypic diagnosis and evolution²¹, but authors did not collect any

hematological data. Previous studies that focused on the correlation between hematological and renal involvements of AE1 mutations were performed in patients carrying recessive mutations (mostly p.G701D) and the specific SAO deletion²²⁻²⁴. Moreover, when RBC anomalies were investigated, authors reported only RBC shape and hemoglobin concentrations. Here, we report data on the transport activity of Band 3 in RBC and on membrane/cytoskeleton relationship, as well as of RBC shape and hemoglobin concentration. Other reports have also shown that *SLC4A1* gene mutations are the main observed anomalies in dRTA not only in Europe²¹, but also in south Asia²⁵. Obvious hematological anomalies appear to be present only if patients carry the specific SAO anomaly²⁶, which is consistent with our findings.

Knowing the precise (RBC) phenotype of patients bearing AE1 mutations could be of high interest at the time of the molecular diagnosis: as stated in the guidelines on the interpretation of molecular data¹⁵, the exponential development of molecular diagnoses leads to the discovery of new “variants”, whom interpretation could be very challenging. As an example, the patient carrying the p.S525F mutation had a class 3 variant (*i.e.* “of uncertain significance”). Interestingly, she had the lowest $k(\text{HCO}_3^-)$ and $P(\text{HCO}_3^-)$ values within the dRTA SAO-. Unfortunately, we did not have enough material to measure $k(\text{Cl}^-)/P(\text{Cl}^-)$. Moreover, the transport of both Cl^- and HCO_3^- in patients carrying a mutation in position 589 appeared to be indistinguishable to the ones of controls. Most of the other mutations seem to have a behavior similar to the one of p.R589H/C. Results from p.S525F remain questionable: RBC phenotype (transport) could lead to interpret it as a differential genotype/phenotype correlation and argue for a functional implication in the phenotype/disease (dRTA) bringing this “variant” to pathogenic, as it occurs in the domain important for the dimerization of the protein.

The recent crystallization structure of Band 3²⁷ and structural analyses⁴ help understanding the differential mechanisms involved in several structural RBC diseases and the wide spectrum of interactions that AE1 develops with other proteins. In RBCs, the full-length AE1 is expressed as oligomers (di- and tetra-mers)¹: the dimers interact with cytosolic enzymes (such as aldolase, glyceraldehyde-3-phosphate dehydrogenase, and carbonic anhydrase) at both the C- and N-terminal part of the protein, while the tetramers are interacting with protein 4.2 and ankyrin, anchoring the complex (thus the membrane) to the cytoskeleton. The interaction between AE1 and ankyrin (thus cytoskeleton) has also been shown in renal cells⁹. This is of particular importance as some mutations

in the *SLC4A1* locus lead to a defect in this specific interaction with the cytoskeleton, then lead to an impaired RBC shape called 'hereditary spherocytosis' ²⁸.

The fact that transport function of kAE1, leading to dRTA is impaired whereas the one of Band 3 is preserved argues for a rescue capacity in RBC. Besides the cytosolic interactions, RBC AE1 also interacts with membrane protein, such as glycophorin A (GPA). Like with cytosolic proteins (such as ankyrin and stomatin ¹⁴), the interaction with GPA can modify or alter the conformation and the function of AE1 ²⁹. More precisely, GPA could act as a protective chaperone by maintaining AE1 membrane expression ³⁰. That is consistent to the fact that in dRTA, kAE1 is less expressed at the membrane and is retained within the Golgi apparatus of kidney cells ³¹. This could be related to other chaperons that avoid its expression (and function) at the α -ICs membrane. Further studies are needed to test whether modifying kAE1 expression by modulating chaperone function(s) could restore renal acidification ability.

Here, we also report differences in the quantitative assessment of Band 3 expression in RBC from SAO patients: when assessed by labeling of extracellular domains of the protein, RBC membranes from SAO patients exhibited a decreased expression of AE1; whereas when assessed by total protein abundance, AE1 expression is not impaired, as previously reported ^{19,20}. This could be related to such an important modification in the conformation of the protein that epitopes detected by immunolabelling could not be recognized, but mobility shift previously reported ¹⁹ has not been detected here.

In conclusion, AE1 dominant mutants associated with dRTA (*i.e.* known to alter transport in kidney) exert normal transport in RBC. Transport in RBC is altered only when SAO mutant is additionally present.

Disclosure / Competing interest

Jean-Philippe Bertocchio, none

Sandrine Genetet, none

Lydie Da Costa, none

Stephen B. Walsh, none

Bertrand Knebelmann, none

Julie Galimand, none

Lucie Bessenay, none

Corinne Guitton, none

Renaud De Lafaille, none

Rosa Vargas-Poussou, none

Dominique Eladari, none

Isabelle Mouro-Chanteloup, none

Acknowledgements

We are grateful to the patients (and their families) affected with dRTA and/or SAO who participated to this study. Authors thank Dr. O. Fenneteau for the RBC images and H. Bourdeau for technical assistance on EMA and ektacytometry.

Funding

J.P.B., S.G., LD.C., and I.M.C. received funding from the laboratory of excellence for Red cells (LABEX GR-Ex)-ANR Avenir-11-LABX-0005-02. DE is funded by grant from l'Agence Nationale de la Recherche (ANR BLANC 14-CE12-0013-01/HYPERSCREEN) and from Philancia.

REFERENCES

1. Cordat E, Reithmeier RA. Structure, function, and trafficking of SLC4 and SLC26 anion transporters. *Curr Top Membr* 2014; **73**: 1-67.
2. Reithmeier RA, Casey JR, Kalli AC, *et al.* Band 3, the human red cell chloride/bicarbonate anion exchanger (AE1, SLC4A1), in a structural context. *Biochim Biophys Acta* 2016; **1858**: 1507-1532.
3. Perrotta S, Gallagher PG, Mohandas N. Hereditary spherocytosis. *Lancet* 2008; **372**: 1411-1426.
4. Rivera-Santiago R, Harper SL, Sriswasdi S, *et al.* Full-Length Anion Exchanger 1 Structure and Interactions with Ankyrin-1 Determined by Zero Length Crosslinking of Erythrocyte Membranes. *Structure* 2017; **25**: 132-145.
5. Da Costa L, Galimand J, Fenneteau O, *et al.* Hereditary spherocytosis, elliptocytosis, and other red cell membrane disorders. *Blood Rev* 2013; **27**: 167-178.
6. Eladari D, Kumai Y. Renal acid-base regulation: new insights from animal models. *Pflugers Arch* 2015; **467**: 1623-1641.
7. Alexander RT, Cordat E, Chambrey R, *et al.* Acidosis and Urinary Calcium Excretion: Insights from Genetic Disorders. *J Am Soc Nephrol* 2016; **27**: 3511-3520.
8. Palazzo V, Provenzano A, Becherucci F, *et al.* The genetic and clinical spectrum of a large cohort of patients with distal renal tubular acidosis. *Kidney Int* 2017; **91**: 1243-1255.
9. Genetet S, Ripoche P, Le Van Kim C, *et al.* Evidence of a structural and functional ammonium transporter RhBG.anion exchanger 1.ankyrin-G complex in kidney epithelial cells. *J Biol Chem* 2015; **290**: 6925-6936.

10. Mumtaz R, Trepiccione F, Hennings JC, *et al.* Intercalated Cell Depletion and Vacuolar H(+)-ATPase Mistargeting in an Ae1 R607H Knockin Model. *J Am Soc Nephrol* 2017; **28**: 1507-1520.
11. Da Costa L, Suner L, Galimand J, *et al.* Diagnostic tool for red blood cell membrane disorders: Assessment of a new generation ektacytometer. *Blood Cells Mol Dis* 2016; **56**: 9-22.
12. Frumence E, Genetet S, Ripoche P, *et al.* Rapid Cl(-)/HCO(-)(3)exchange kinetics of AE1 in HEK293 cells and hereditary stomatocytosis red blood cells. *Am J Physiol Cell Physiol* 2013; **305**: C654-662.
13. King MJ, Behrens J, Rogers C, *et al.* Rapid flow cytometric test for the diagnosis of membrane cytoskeleton-associated haemolytic anaemia. *Br J Haematol* 2000; **111**: 924-933.
14. Genetet S, Desrames A, Chouali Y, *et al.* Stomatin modulates the activity of the Anion Exchanger 1 (AE1, SLC4A1). *Sci Rep* 2017; **7**: 46170.
15. Richards S, Aziz N, Bale S, *et al.* Standards and guidelines for the interpretation of sequence variants: a joint consensus recommendation of the American College of Medical Genetics and Genomics and the Association for Molecular Pathology. *Genet Med* 2015; **17**: 405-424.
16. DuBose TD, Jr., Caflich CR. Validation of the difference in urine and blood carbon dioxide tension during bicarbonate loading as an index of distal nephron acidification in experimental models of distal renal tubular acidosis. *The Journal of clinical investigation* 1985; **75**: 1116-1123.
17. Wrong O, Davies HE. The excretion of acid in renal disease. *The Quarterly journal of medicine* 1959; **28**: 259-313.

18. Walsh SB, Shirley DG, Wrong OM, *et al.* Urinary acidification assessed by simultaneous furosemide and fludrocortisone treatment: an alternative to ammonium chloride. *Kidney Int* 2007; **71**: 1310-1316.
19. Bruce LJ, Wrong O, Toye AM, *et al.* Band 3 mutations, renal tubular acidosis and South-East Asian ovalocytosis in Malaysia and Papua New Guinea: loss of up to 95% band 3 transport in red cells. *Biochem J* 2000; **350 Pt 1**: 41-51.
20. Schofield AE, Reardon DM, Tanner MJ. Defective anion transport activity of the abnormal band 3 in hereditary ovalocytic red blood cells. *Nature* 1992; **355**: 836-838.
21. Lopez-Garcia SC, Emma F, Walsh SB, *et al.* Treatment and long-term outcome in primary distal renal tubular acidosis. *Nephrol Dial Transplant* 2019; **34**: 981-991.
22. Khositseth S, Sirikanaerat A, Khoprasert S, *et al.* Hematological abnormalities in patients with distal renal tubular acidosis and hemoglobinopathies. *Am J Hematol* 2008; **83**: 465-471.
23. Khositseth S, Sirikanerat A, Wongbenjarat K, *et al.* Distal renal tubular acidosis associated with anion exchanger 1 mutations in children in Thailand. *Am J Kidney Dis* 2007; **49**: 841-850 e841.
24. Khositseth S, Bruce LJ, Walsh SB, *et al.* Tropical distal renal tubular acidosis: clinical and epidemiological studies in 78 patients. *QJM* 2012; **105**: 861-877.
25. Park E, Cho MH, Hyun HS, *et al.* Genotype-Phenotype Analysis in Pediatric Patients with Distal Renal Tubular Acidosis. *Kidney Blood Press Res* 2018; **43**: 513-521.
26. Besouw MTP, Bienias M, Walsh P, *et al.* Clinical and molecular aspects of distal renal tubular acidosis in children. *Pediatr Nephrol* 2017; **32**: 987-996.

27. Arakawa T, Kobayashi-Yurugi T, Alguel Y, *et al.* Crystal structure of the anion exchanger domain of human erythrocyte band 3. *Science* 2015; **350**: 680-684.
28. Low PS, Zhang D, Bolin JT. Localization of mutations leading to altered cell shape and anion transport in the crystal structure of the cytoplasmic domain of band 3. *Blood Cells Mol Dis* 2001; **27**: 81-84.
29. Kalli AC, Reithmeier RAF. Interaction of the human erythrocyte Band 3 anion exchanger 1 (AE1, SLC4A1) with lipids and glycophorin A: Molecular organization of the Wright (Wr) blood group antigen. *PLoS Comput Biol* 2018; **14**: e1006284.
30. Williamson RC, Toye AM. Glycophorin A: Band 3 aid. *Blood Cells Mol Dis* 2008; **41**: 35-43.
31. Patterson ST, Reithmeier RA. Cell surface rescue of kidney anion exchanger 1 mutants by disruption of chaperone interactions. *J Biol Chem* 2010; **285**: 33423-33434.
32. Bruce LJ, Cope DL, Jones GK, *et al.* Familial distal renal tubular acidosis is associated with mutations in the red cell anion exchanger (Band 3, AE1) gene. *The Journal of clinical investigation* 1997; **100**: 1693-1707.
33. Quilty JA, Li J, Reithmeier RA. Impaired trafficking of distal renal tubular acidosis mutants of the human kidney anion exchanger kAE1. *Am J Physiol Renal Physiol* 2002; **282**: F810-820.
34. Cordat E, Kittanakom S, Yenchitsomanus PT, *et al.* Dominant and recessive distal renal tubular acidosis mutations of kidney anion exchanger 1 induce distinct trafficking defects in MDCK cells. *Traffic* 2006; **7**: 117-128.
35. Zhang Z, Liu KX, He JW, *et al.* Identification of two novel mutations in the SLC4A1 gene in two unrelated Chinese families with distal renal tubular acidosis. *Arch Med Res* 2012; **43**: 298-304.

36. Rungroj N, Devonald MA, Cuthbert AW, *et al.* A novel missense mutation in AE1 causing autosomal dominant distal renal tubular acidosis retains normal transport function but is mistargeted in polarized epithelial cells. *J Biol Chem* 2004; **279**: 13833-13838.
37. Tanphaichitr VS, Sumboonnanonda A, Ideguchi H, *et al.* Novel AE1 mutations in recessive distal renal tubular acidosis. Loss-of-function is rescued by glycophorin A. *The Journal of clinical investigation* 1998; **102**: 2173-2179.
38. Kittanakom S, Cordat E, Akkarapatumwong V, *et al.* Trafficking defects of a novel autosomal recessive distal renal tubular acidosis mutant (S773P) of the human kidney anion exchanger (kAE1). *J Biol Chem* 2004; **279**: 40960-40971.
39. Bracher NA, Lyons CA, Wessels G, *et al.* Band 3 Cape Town (E90K) causes severe hereditary spherocytosis in combination with band 3 Prague III. *Br J Haematol* 2001; **113**: 689-693.
40. Ashton EJ, Legrand A, Benoit V, *et al.* Simultaneous sequencing of 37 genes identified causative mutations in the majority of children with renal tubulopathies. *Kidney Int* 2018; **93**: 961-967.

Tables

Table 1. Characteristics of included patients at diagnosis.

Patients	Mutation	Gender	Age (y)	Hb (g/L)	CrP (μ M)	eGFR (mL/min/1.73m ²)	CO ₂ t (mM)	Nephrolithiasis	Nephrocalcinosis	Familial history	Dynamic test	Known RBC anomaly	Bone demineralization
1	p.R589H	M	9	NA	41	92	8	Y	N	Y	N	N	Y
2	p.R589H	F	33	11.5	94	61	20	Y	Y	Y	N	N	N
3	p.R589H	M	45	14.9	115	57	21	Y	Y	Y	Y	N	N
4	p.R589C	F	25	13.2	73	89	22	Y	Y	Y	Y	Iron deficiency	N
5	p.R589H	F	2	13.0	71	>90	21	Y	Y	Y	N	N	Y
6	p.E906*	M	30	17.5	142	52	23	Y	Y	Y	Y	Polycythemia	N
7	p.S613F	F	20	12.5	76	74	23	Y	Y	Y	N	N	N
8	p.R589C	F	2	11.1	36	103	13	N	Y	N	N	Elliptocytes	Y
9	p.R589C	F	1	NA	NA	NA	NA	Y	Y	N	Y	N	NA
10	p.D905dup	M	9	NA	75	71	NA	Y	Y	N	Y	N	NA
11	p.E906K	M	44	13.1	80	103	23	Y	N	Y	Y	N	N
12	p.G609R	M	34	9.4	196	36	8	Y	Y	Y	N	N	NA
13	p.S525F	F	14	NA	62	125	14	Y	Y	N	Y	N	N
14	del27/p.G701D	F	2	13.0	88	74	19	Y	Y	N	Y	Anisocytes, macrocytes, stomatocytes	N
15	p.E90K/p.T581D/del27	M	9	13.0	40	77	15	N	Y	N	N	Ovalocytes	Y

Distal renal tubular acidosis was assessed by a dynamic test (Δ U-B_{PCO2}), acute acid load, and/or the furosemide-fludrocortisone test) in 8 of them. All experienced nephrolithiasis and/or nephrocalcinosis. Five patients had known red blood cell (RBC) morphological anomalies. y: years; Hb: hemoglobin; CrP: creatinemia; eGFR: estimated glomerular filtration rate; M: male; F: female; Y: yes; N: no; NA: information not available

Table 2. Mutations in the *SLC4A1* gene exerted by included patients.

Patient	Gender	Age	Short name mutation	Nucleotide	Protein	Type of mutation	Localization	Ref.	Exon	<i>In vitro</i> data ref.	Class ACMG 2015
1	M	13	p.R589C	c.1765C>T	p.Arg589Cys	5	TM6	32	14	32, 33	PS3, PS4, PM1, PM2, PP3, PP5
2	F	41	p.R589H	c.1766G>A	p.Arg589His	5	TM6	32	14	32-34	PS3, PS4, PM1, PM2, PP3, PP5
3	M	70	p.R589H	c.1766G>A	p.Arg589His	5	TM6	32	14	32-34	PS3, PS4, PM1, PM2, PP3, PP5
4	F	30	p.R589C	c.1765C>T	p.Arg589Cys	5	TM6	32	14	32, 33	PS3, PS4, PM1, PM2, PP3, PP5
5	F	22	p.R589H	c.1766G>A	p.Arg589His	5	TM6	32	14	32-34	PS3, PS4, PM1, PM2, PP3, PP5
6	M	34	p.E906*	c.2716G>T	p.Glu906*	5	C-ter	21	20	Not described	PVS1, PM1, PM2
7	F	55	p.S613F	c.1838C>T	p.Ser613Phe	5	TM7	32	15	32, 34	PS3, PM1, PM2, PP3, PP5
8	F	15	p.R589C	c.1765C>T	p.Arg589Cys	5	TM6	32	14	32, 33	PS3, PS4, PM1, PM2, PP3, PP5
9	F	28	p.R589C	c.1765C>T	p.Arg589Cys	5	TM6	32	14	32, 33	PS3, PS4, PM1, PM2, PP3, PP5
10	M	52	p.D905dup	c.2715_2717 dup	p.Asp905dup	4	C-ter	35	20	Not described	PM1, PM2, PM4, PP5
11	M	47	p.E906K	c.2716G>A	p.Glu906Lys	4	C-ter	Not described	20	Not described	PM1, PM2, PM5
12	M	29	p.G609R	c.1825G>A	p.Gly609Arg	5	TM7	36	15	36	PS3, PM1, PM2, PP3, PP5
13	F	28	p.S525F	c.1574C>T	p.Ser525Phe	3	TM5	Not described	13	Not described	PM1, PM2, PP3
Ovalocytosis											
14	F	25	p.G701D	c.2102G>A	p.Gly701Asp	5	ICL8-9	37	17	34, 37, 38	PS3, PM1, PM2, PP3, PP5
			del27	c.1199_1225 del	p.Ala400_Ala 408del	4	TM1	26	11	Not described	PM2, PM4, PP3, PP5
15	M	11	p.E90K	c.268G>A	p.Glu90Lys	4	N-ter	39	5	Not described	PS3, PM1, PM2, PP5

p.T581D	c.1742C>A	p.Thr581Asn	3	TM6	40	14	Not described	PM1, PM2
del27	c.1199_1225 del	p.Ala400_Ala 408del	4	TM1	26	11	Not described	PM2, PM4, PP3, PP5

Eighteen (12 different) gene mutations were identified in 15 patients. Two were predicted *in silico* whereas 10 were previously reported. Thirteen patients had dominant distal renal tubular acidosis (dRTA). Three mutations were located at the C-terminal (C-term) domain, while 1 was found at the N-terminal (N-term) domain, 1 in the intracellular loop (ICL) between transmembrane domain (TM) 8 and TM9. Eight, 2, and 2 were found in TM6, TM7, and TM1, respectively. Following the American college of medical genetics (ACMG) recommendations published previously ¹⁵, variants were classified into five categories (class 1: benign; class 2: likely benign; class 3: uncertain significance; class 4: likely pathogenic and class 5: pathogenic) based on several criteria including population data, computational data, functional data, and segregation data. These criteria are weighted as very strong (PVS1), strong (PS1–4); moderate (PM1–6), or supporting (PP1–5). The mutations previously reported are presented with their reference (ref.), as well as the references of the *in vitro* characterization of the mutation showing their pathogenicity.

Table 3. Biology at inclusion.

Patients	Short name mutation	Age	Gender	WBC (10 ⁹ /L)	RBC (10 ¹² /L)	Hb (g/dL)	MCV (fL)	Platelets (10 ⁹ /L)	MCH (pg/cell)	MCH (g/L)	Reticulocytes (10 ⁹ /L)	Elmax	Omin (Osm/kgH ₂ O)	Ohyper (Osm/kgH ₂ O)
1	p.R589H	13	M	6.72	4.80	13.9	84.4	274	29.0	34.3	42.7	0.55	142	404
2	p.R589H	41	F	10.62	5.25	14.5	93.0	257	27.6	29.7	81.9	0.56	161	457
3	p.R589H	70	M	6.17	5.32	16.0	99.1	254	30.1	30.4	64.9	0.56	155	447
4	p.R589C	30	F	5.58	4.41	13.6	99.8	204	30.8	30.9	50.7	0.58	160	443
5	p.R589H	22	F	11.38	4.81	13.9	95.0	252	28.9	30.4	46.7	0.56	154	446
6	p.E906*	34	M	8.11	5.91	17.3	97.0	271	29.3	30.2	66.8	0.55	171	452
7	p.S613F	55	F	6.28	3.8	12.0	106.3	170	31.6	29.7	35.3	0.57	164	457
8	p.R589C	15	F	9.10	4.74	11.9	77.0	407	25.1	32.6	30.3	0.52	120	385
9	p.R589C	28	F	6.98	3.96	12.1	87.9	189	34.8	30.6	84.4	0.55	150	414
10	p.D905dup	52	M	5.29	5.03	15.0	90.3	176	29.8	33.0	61.9	0.55	156	420
11	p.E906K	47	M	5.66	4.47	12.9	94.2	272	28.9	30.6	80.9	0.58	154	452
12	p.G609R	29	M	7.81	4.13	11.5	87.9	180	27.8	31.7	73.9	0.57	144	452
13	p.S525F	28	F	4.57	4.59	13.3	87.1	240	29.0	33.3	47.7	0.58	155	456
Ovalocytosis														
14	del27/p.G701D	25	F	10.86	3.58	14.4	111.7	488	40.2	36.0	190.8	0.29	79	240
15	del27/p.E90K/ p.T581D	11	M	9.32	5.62	12.8	73.2	499	22.7	31.0	120.6	0.00	NA	NA
median		29		6.98	4.74	13.6	93.0	254	29.0	30.9	64.9	0.56	155	447
Q1		24		5.92	4.27	12.5	87.5	197	28.4	30.4	47.2	0.55	146	420
Q3		44		9.21	5.14	14.5	98.1	273	30.5	32.8	81.4	0.57	159	452

No patient exhibited severe anemia at the time of inclusion. WBC: white blood cells count. RBC: red blood cell count. Hb: hemoglobin. MCV: mean corpuscular volume in femtoliter (fL). MCH: mean corpuscular hemoglobin. Omin: reflects the surface area/volume ratio and corresponds to the osmolality at the minimal deformability in hypoosmolar area, or at the osmolality when 50% of the red cells hemolyzed during the regular osmotic resistance test. Elmax:

corresponds to the maximal deformability index or elongation index (EI). Ohyper: corresponds to the osmolality at half of the DI_{max} and reflects the hydration state of the RBC. NA: not appropriate. Q1: first quartile. Q3: third quartile.

Captions of figures

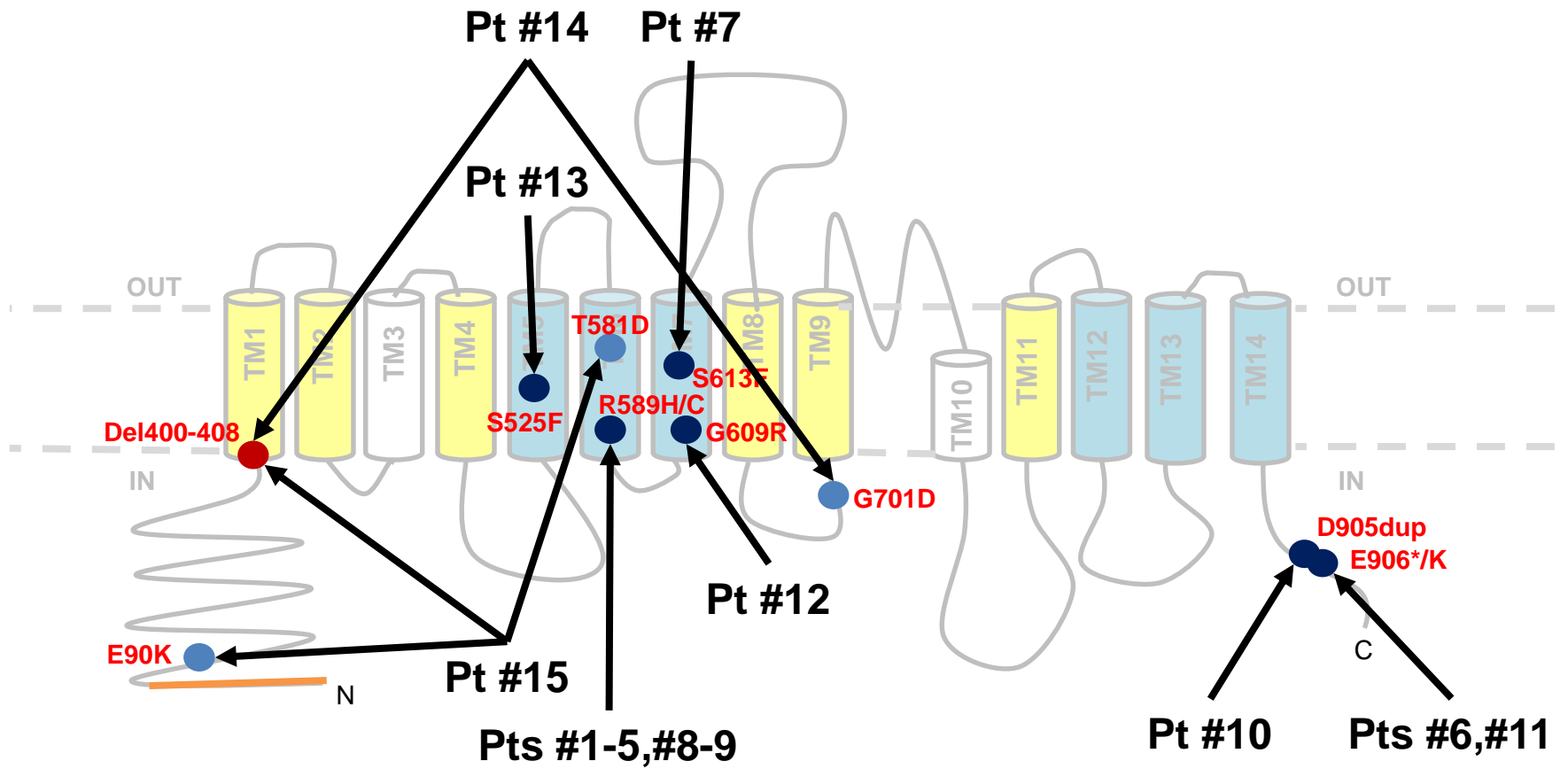
Figure 1. Localizations of mutations carried by included patients. This 2D representation of anion exchanger 1 (AE1) protein inserted into the cell membrane shows the precise localization of the 12 different mutations identified in our cohort of patients (Pt). Red dot shows the typical deletion of 27 base pairs (*i.e.* 9 aminoacids) found during South Asian Ovalocytosis (SAO). Blue dots show the mutations involved in distal renal tubular acidosis (dRTA): light and dark ones are recessive and dominant mutations, respectively. In orange, we represent the 65 missing aminoacids at the N-terminal part of the kidney isoform of AE1 (kAE1). The 14 transmembrane domains (TM) belonging to the core and the gate are colored in yellow and cyan, respectively ²⁷.

Figure 2. Reb blood cells from included patients. Up: Blood smears after May-Grünwald Giemsa coloration (MGG) in healthy controls, in patients exerting a dominant mutation in the *SLC4A1* gene leading to distal renal tubular acidosis (dRTA SAO-), and patients exerting a mutation in the *SLC4A1* gene leading to South Asian Ovalocytosis (SAO) in addition to the one leading to dRTA (dRTA SAO+). At the bottom: Ektacytometry curves revealed a dramatic decrease in the elongation indexes only in the dRTA SAO+ affected patients, while there were normal in the dRTA SAO- patients.

Figure 3. Transports of HCO₃⁻ and Cl⁻ in ghosts from patients with mutations in AE1 gene and controls. From circulating red blood cells (RBC), ghosts were resealed with pyranine to measure volume and membrane surface (**Panel A**). Relative values of transport (k) of both HCO₃⁻ (**Panel B**) and Cl⁻ (**Panel C**) were significantly decreased in patients exerting a mutation in the *SLC4A1* gene leading to South Asian Ovalocytosis (SAO) in addition to the one leading to dRTA (dRTA SAO+), as compared to the other ones, as well as controls. HCO₃⁻ and Cl⁻ k and permeability (P) were correlated among each other and were strongly different in dRTA SAO+ as compared to the other (**Panels D and E**).

Figure 4. AE1 protein expression at RBC membrane. The membrane expression of AE1 was studied in ghosts from red blood cells by flow cytometry with 3 different probes: EMA, Bric6, and Diego B (**Panel A**). Those 3 probes recognize 3 different extracellular domains of the AE protein (**Panel B**). The Coomassie

staining is shown in **Panel C** with its intensity. The quantifications (**Panel D**) of the intensity of Band 3 (top) and Band 3/full lane (bottom) did not show any difference.

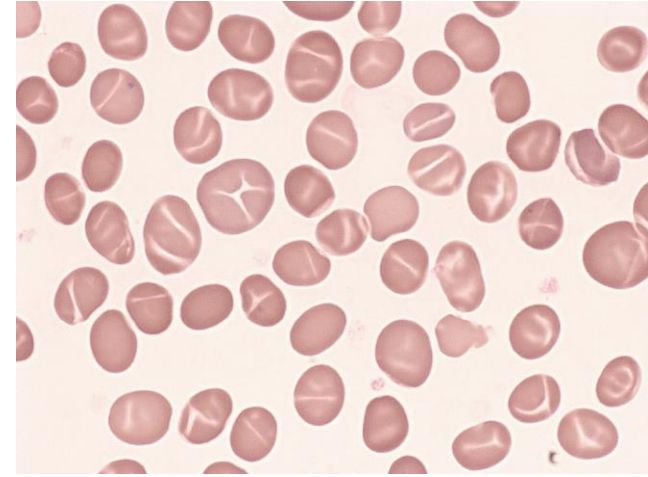
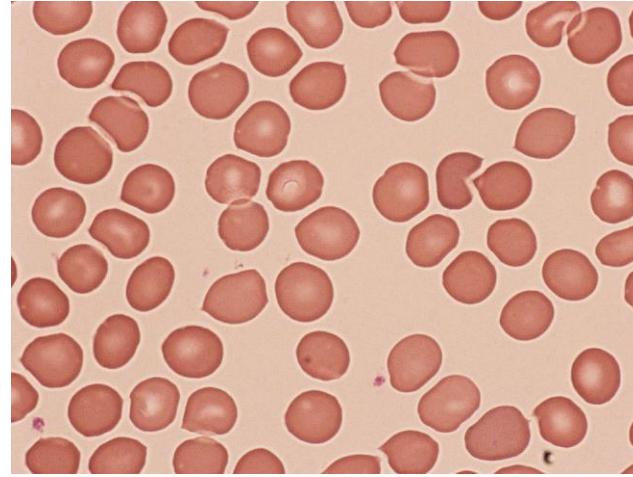
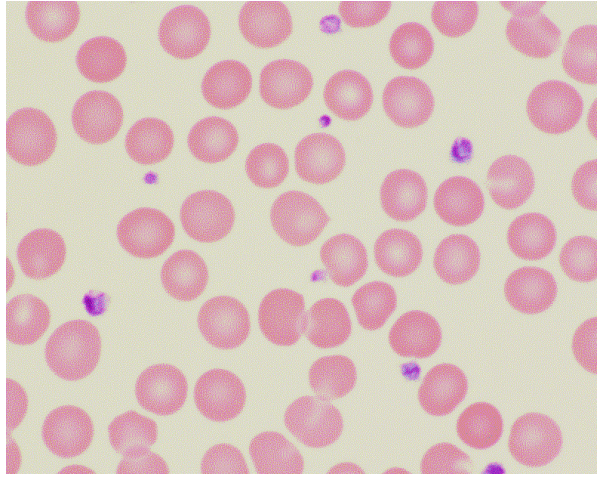


Controls

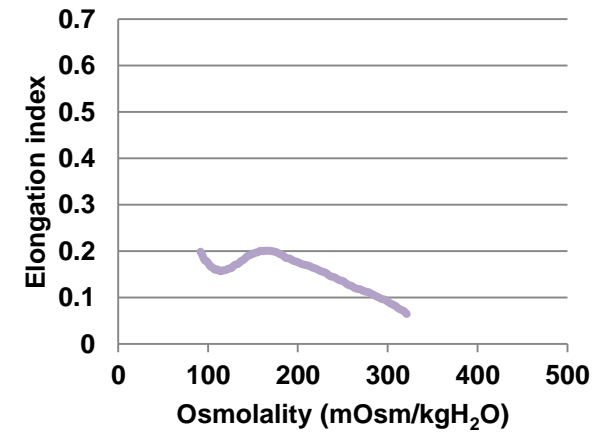
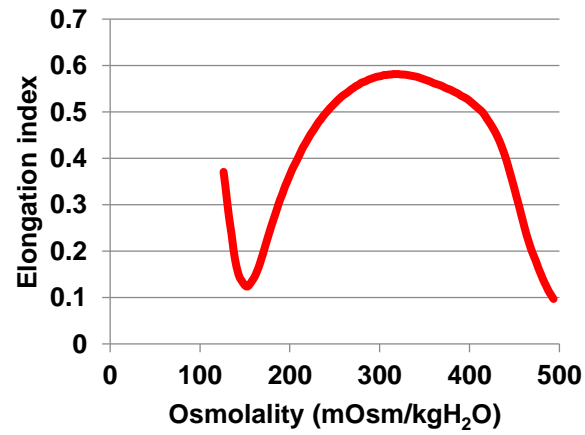
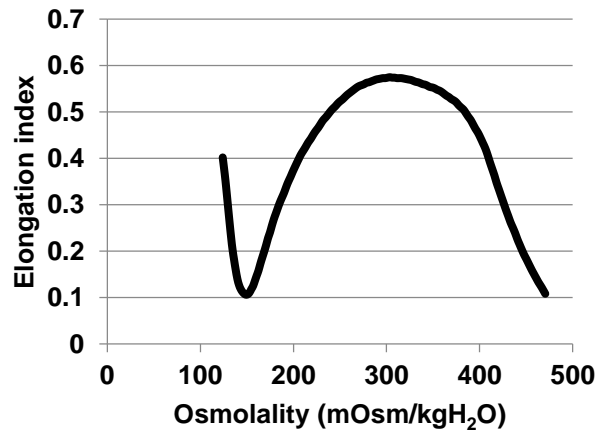
dRTA SAO-

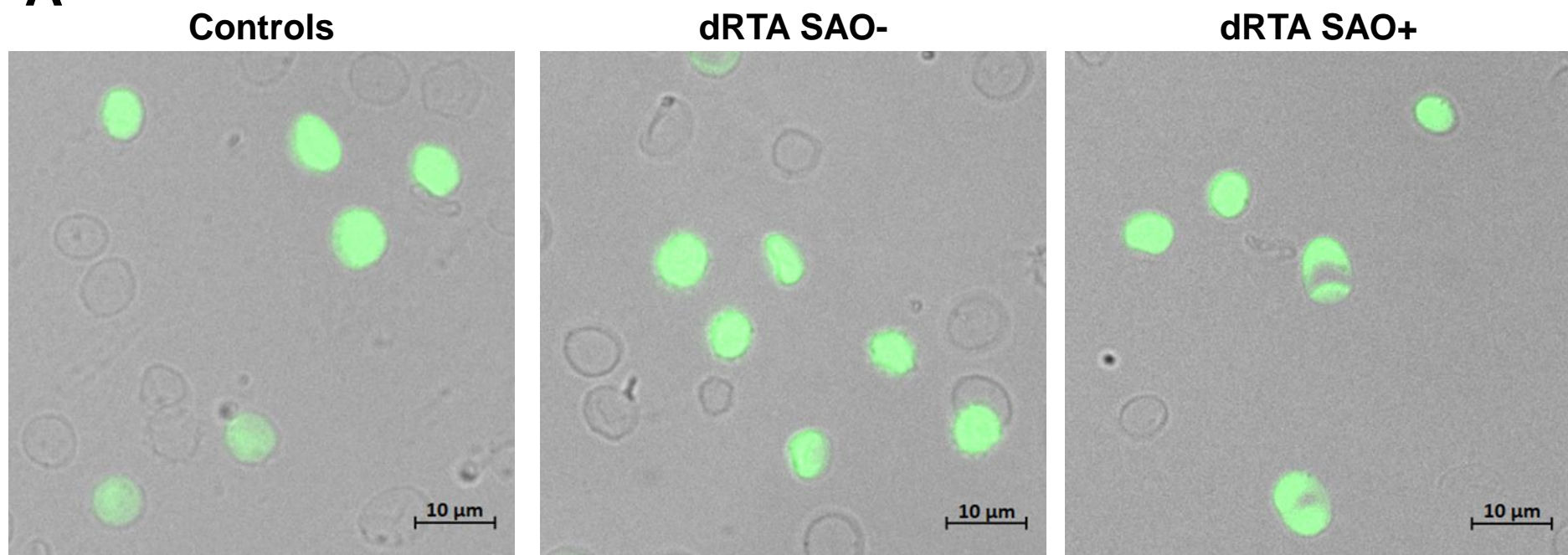
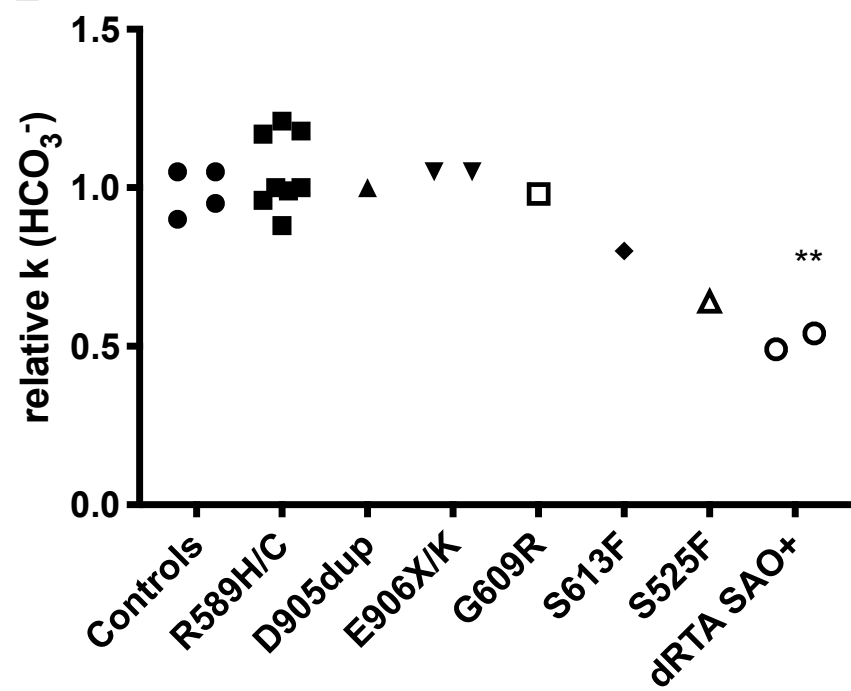
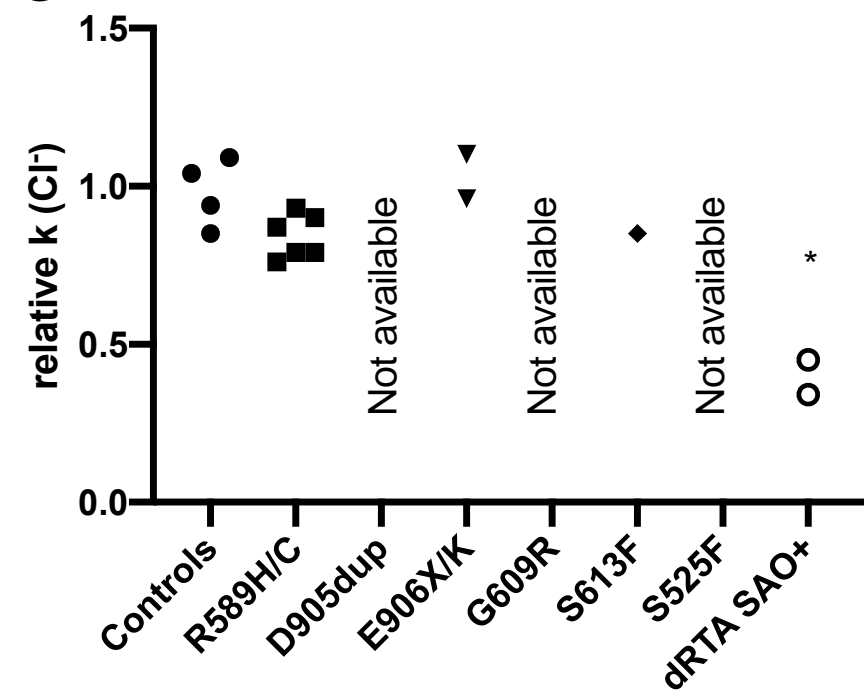
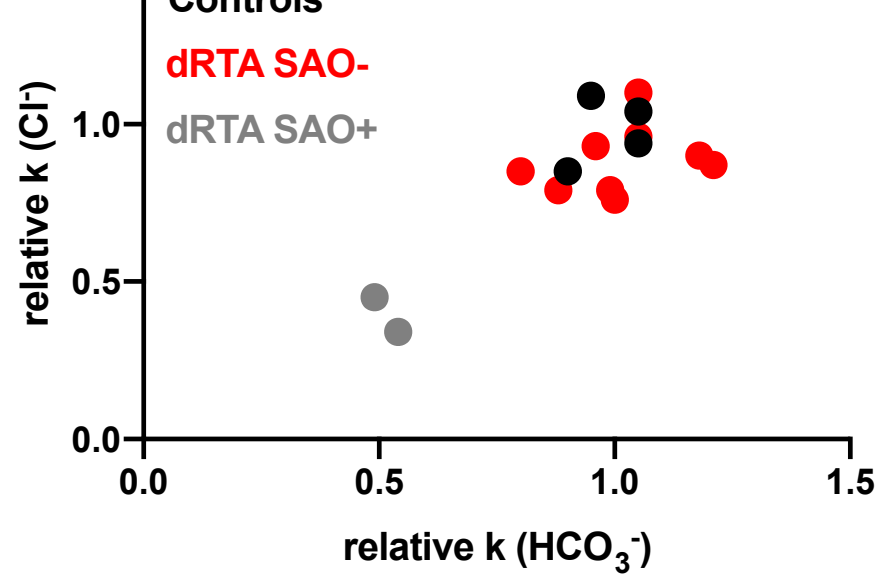
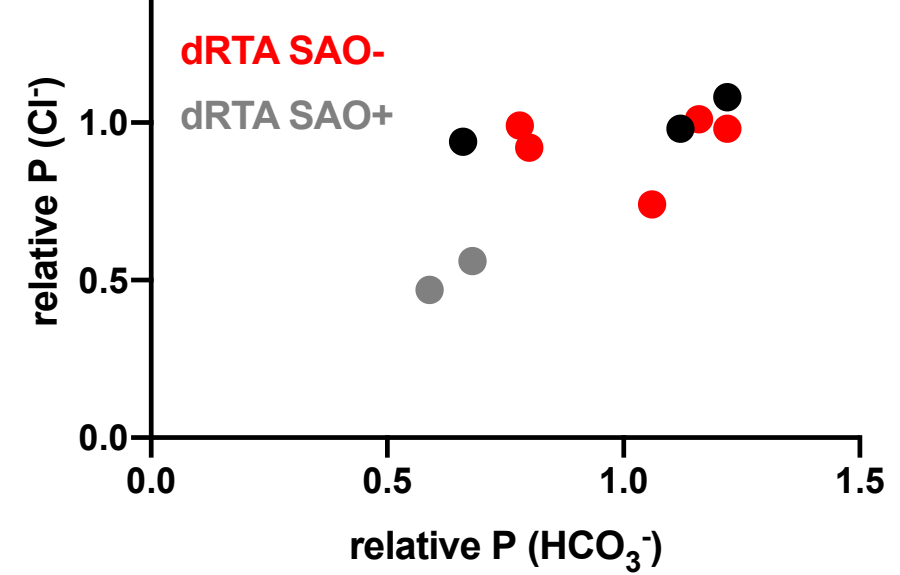
dRTA SAO+

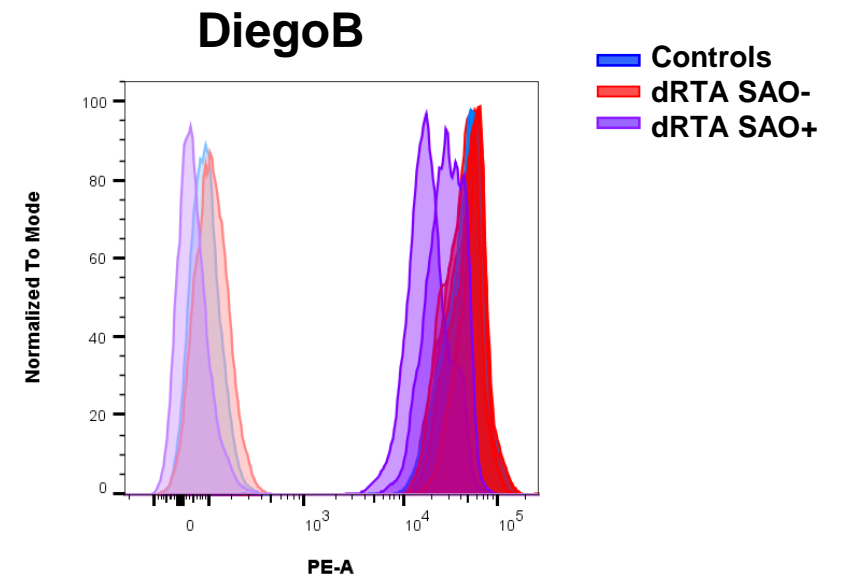
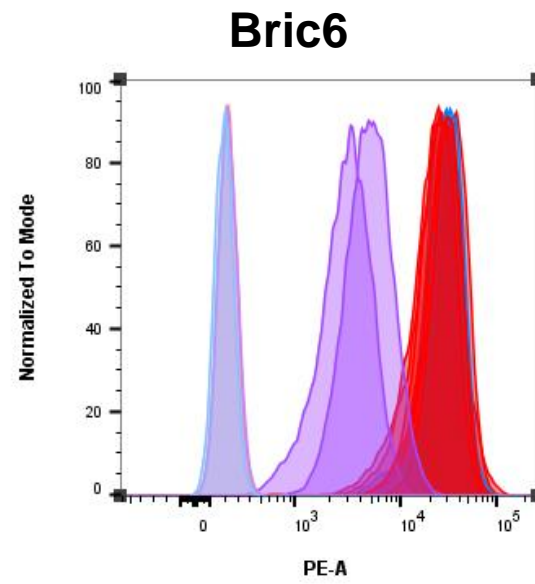
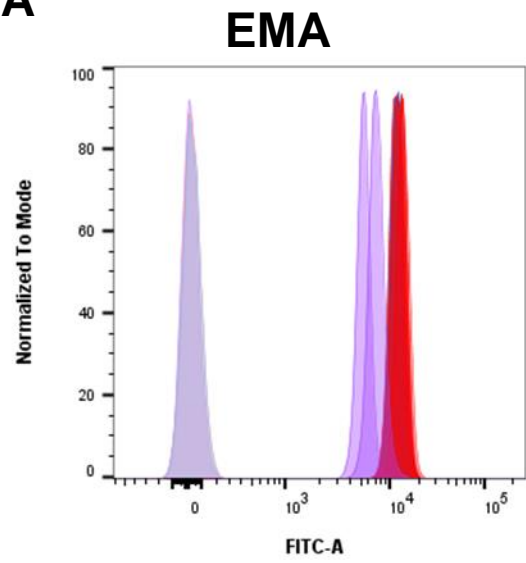
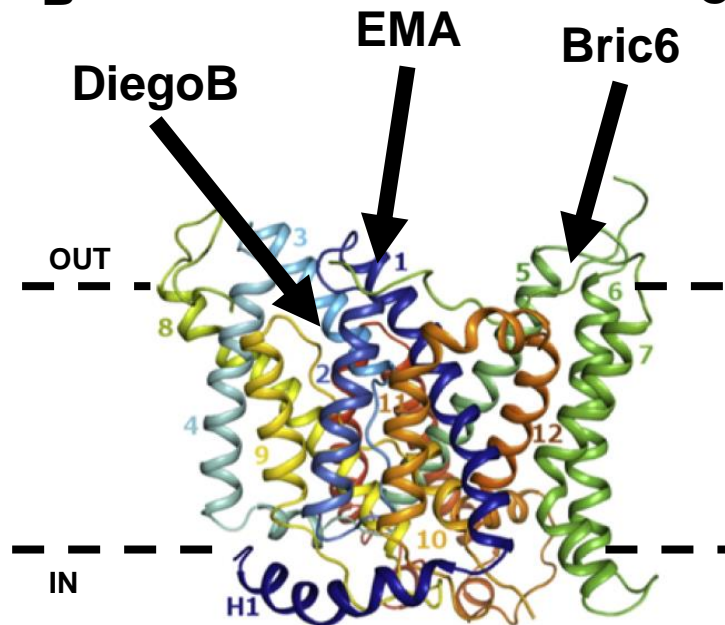
Blood smear



Ektacytometry



A**B****C****D****E**

A**B****C**